DOI: 10.1109/ISGT-Asia.2015.7387067

URL: http://ieeexplore.ieee.org/xpls/abs_all.jsp?arnumber=7387067&tag=1

Thomas Geury, Sonia Pinto and Johan Gyselinck
Université Libre de Bruxelles
Avenue Franklin Roosevelt 50 (CP165/52)
B-1050 Brussels
Belgium

Phone: +32 (0) 2 650 26 61
Fax: +32 (0) 2 650 26 53
Email: thomas.geury@ulb.ac.be

An Indirect Matrix Converter-based Unified Power Quality Conditioner for a PV inverter with enhanced Power Quality functionality

Thomas Geury[1,2,3], Sonia Pinto[2], Johan Gyselinck[3], Patrick Wheeler[4]
[1] F.R.I.A. scholarship student, email: thomas.geury@ulb.ac.be
[2] INESC-ID Lisboa, IST – ULisbon, Lisbon, Portugal
[3] BEAMS Energy, EPB – ULB, Brussels, Belgium
[4] Department of Electrical and Electronic Engineering, University of Nottingham, Nottingham, UK

***Abstract*—This paper introduces an Indirect Matrix Converter (IMC)-based Unified Power Quality Conditioner topology for a Photovoltaic (PV) system and sensitive load, with enhanced Power Quality functionalities. In particular, the proposed system is able to compensate grid voltage sags, swells and harmonics in the sensitive load, and non-linear load current harmonics in the Low-Voltage (LV) grid, in addition to the common PV inverter functionalities. The modulation of the shunt converter is developed specifically to control the PV array current and the grid currents amplitude, as opposed to the common IMC modulation methods. The IMC modulation is synchronized with the series inverter modulation in order for the system to operate as a whole. Simulation results are presented to confirm the proper operation of the system under a variety of operating conditions.**

***Index Terms*—Matrix converters, Photovoltaic systems, Power harmonic filters, Power Quality, Space vector PWM.**

I. INTRODUCTION

In recent years, new power converter topologies for Photovoltaic (PV) systems have been proposed to improve the efficiency or the reliability, reduce the number of components, allow for a better management of the production or add enhanced functionality to the usual Maximum Power Point Tracking (MPPT) and Power Factor (PF) regulation. In particular, the Power Quality (PQ) issues on the Low-Voltage (LV) grid are crucial with the increasing use of power electronics-based equipment and distributed resources.

In this context, standards IEEE 1547, IEC 61727 and VDE 0126-1-1 (Germany) regulate the PV connection to the LV grid while other standards aim specifically at the current harmonics production (IEEE 61000-3-2) or the voltage quality with sags, swells and harmonics (EN 50160, Europe) [1]. The mitigation of non-linear load current harmonics by adding Active Power Filter (APF) capability to the PV converter has been developed [2]. However, PV systems are commonly disconnected from the grid during voltage sags or swells, causing extra stress on the grid and potentially leading to power imbalance and instability. Thus, standards requiring the distributed generation units to actively support the grid, such as VDE-AR-N 4105 (Germany), are being developed.

The developed system uses a Unified Power Quality Conditioner (UPQC)-based topology [3], [4], with shunt and series converters, in order to compensate these current- and voltage-related issues, respectively. The PV array is inserted in the DC link [4]–[6] for the steady supply of energy and a better integration of distributed resources on the grid. This contrasts with the shunt converters which can be used for voltage sags and swells with reactive power compensation [5]–[7] or adjustment of the active power production [8]. The latter topology has several drawbacks with limited compensation capabilities; the UPQC-based system is more appropriate to the voltage compensations and is more flexible.

In this paper it is proposed to use an Indirect Matrix Converter (IMC) instead of the more traditional Voltage Source Inverter (VSI) for the series and shunt converters of a UPQC, removing the bulky storage capacitor in the DC link. This provides the advantages of Matrix Converters (MCs) and improves the quality and compactness of the system [9] while having access to a 'virtual DC link' to connect the PV array. The shunt converter acts as a step-up converter, removing the need for the common DC/DC converter in VSI topologies.

The objective of this paper is to adapt the modulation of the IMC to allow the insertion of a PV array in its 'virtual DC link' and control the resulting UPQC-based topology for compensating PQ issues. The modulation of the IMC is detailed in the second section. Next, the control of the system is briefly presented. Simulation results are also presented to confirm the system operates properly.

II. DESCRIPTION OF THE SYSTEM

The topology of the system is described and the IMC is presented in detail with the relevant notations.

A. Topology description

In a UPQC, the series APF compensates the voltage-related issues, such as supply voltage sags, swells and harmonics, while the shunt APF compensates the current-

related ones, such as load current harmonics and reactive current compensation. An IMC is here used to form the UPQC-based topology and the PV array is connected to the 'virtual DC link' with the usual PV functionalities of PF regulation and MPPT, resulting in the system shown in Fig. 1.

The grid voltages are compared to their references to generate the compensation voltage references to be reproduced by the series inverter, with an LC filter, such that the load voltages are as required.

$$v_{\mathrm{nl,abc}} = v_{\mathrm{abc}} - v_{\mathrm{ABC}} \tag{1}$$

The grid currents are measured and controlled to remain sinusoidal using the shunt converter AC currents to compensate the load current harmonics, such that

$$i_{\mathrm{abc}} = i_{\mathrm{abc}}^{''} - i_{\mathrm{nl,abc}} . \tag{2}$$

The DC link current flowing through the shunt converter is

$$I_{\mathrm{dc}} = I_{\mathrm{PV}} + I_{\mathrm{dc}}^{'} , \tag{3}$$

where $I_{\mathrm{dc}}^{'}$ is the current from the series inverter. Most of the power produced by the PV array flows through the shunt converter to the load or to the grid.

B. Indirect Matrix Converter

The IMC, without considering the non-linear load and the UPQC topology, is shown in Fig. 2. It is identical to a MC in principle and features the same number of switches (18 IGBTs and 18 diodes) but a 'virtual DC link' is made accessible since it does not perform direct AC/AC conversion [10]–[12]. Thus, it can be modelled as the combination of a rectifier or 3x2 MC and an inverter, represented by the switching vectors

$$\mathbf{S}_1 = \begin{bmatrix} S_{11} & S_{12} & S_{13} \\ S_{21} & S_{22} & S_{23} \end{bmatrix} , \ \mathbf{S}_2 = \begin{bmatrix} S_{\mathrm{AA}} & S_{\mathrm{AB}} & S_{\mathrm{AC}} \\ S_{\mathrm{BA}} & S_{\mathrm{BB}} & S_{\mathrm{BC}} \end{bmatrix} , \tag{4}$$

respectively [9].

The rectifier AC side is of the voltage-source type and the inverter one of the current-source type, such that the DC bus voltage and current are determined by the rectifier AC voltages and inverter AC currents, respectively. Thus, the inverter voltages v_{sABC} are obtained based on the rectifier voltages v_{sabc} (5), and the rectifier currents i_{sabc} are similarly obtained based on the inverter currents i_{sABC} (5).

$$\mathbf{v}_{\mathrm{sABC}} = \mathbf{S}_1 \mathbf{S}_2^T \mathbf{v}_{\mathrm{sabc}} \ , \ \mathbf{i}_{\mathrm{sabc}} = \mathbf{S}_2 \mathbf{S}_1^T \mathbf{i}_{\mathrm{sABC}} \tag{5}$$

For further developments, the AC voltages and currents are directly considered at the output of the filters, such that v_{ABC} and i_{abc} are considered instead of v_{sABC} and i_{sabc}, respectively, for the sake of clarity. The filter dynamics will be considered when sizing the controllers.

The fundamental components of the rectifier AC voltages and currents are defined by (6), where ϕ_1 is the displacement angle and $(k, j) = \{(\mathrm{a},1),(\mathrm{b},2),(\mathrm{c},3)\}$.

$$\begin{aligned} v_k &= \hat{V}_1 \cos\left(\omega_1 t - (j-1)\tfrac{2\pi}{3}\right) \\ i_k &= \hat{I}_1 \cos\left(\omega_1 t - (j-1)\tfrac{2\pi}{3} + \phi_1\right) \end{aligned} \tag{6}$$

Similarly, the fundamental components of the inverter AC variables are defined by (7), where ϕ_2 is the displacement angle, φ_2 is the phase shift between the two converters AC voltages and $(k, j) = \{(\mathrm{A},1),(\mathrm{B},2),(\mathrm{C},3)\}$.

$$\begin{aligned} v_k &= \hat{V}_2 \cos\left(\omega_2 t - (i-1)\tfrac{2\pi}{3} + \varphi_2\right) \\ i_k &= \hat{I}_2 \cos\left(\omega_2 t - (i-1)\tfrac{2\pi}{3} + \phi_2 + \varphi_2\right) \end{aligned} \tag{7}$$

For the sake of clarity, φ_2 is considered null in the following analyses. The voltages and currents can also be represented as space vectors in the αβ0 frame, using the power-invariant Concordia transformation.

The switching states of the series and shunt converters are represented in Table I and Table II, respectively.

III. Modulation of the Indirect Matrix Converter

The modulation of the IMC is achieved using Space Vector Modulation (SVM) with Pulse Width Modulation (PWM) [12]–[16]. The objective is to reproduce the references that are set for the AC voltages of the series inverter and the AC currents of the 3x2 MC. This is studied first considering separate modulations for the two parts of the IMC. Then, the converter is considered as a whole by synchronizing the modulations and adapting them to introduce the PV array in the DC link and control the PV array current.

A. Series inverter modulation

The modulation of the series inverter is first considered with a constant voltage source V_{dc} in the DC link.

The AC voltages are obtained in Table I in function of the switching vectors, and are also represented by space vectors $\vec{v}_{\mathrm{s}}$. These are shown in Fig. 3 in the two-axis non-rotating

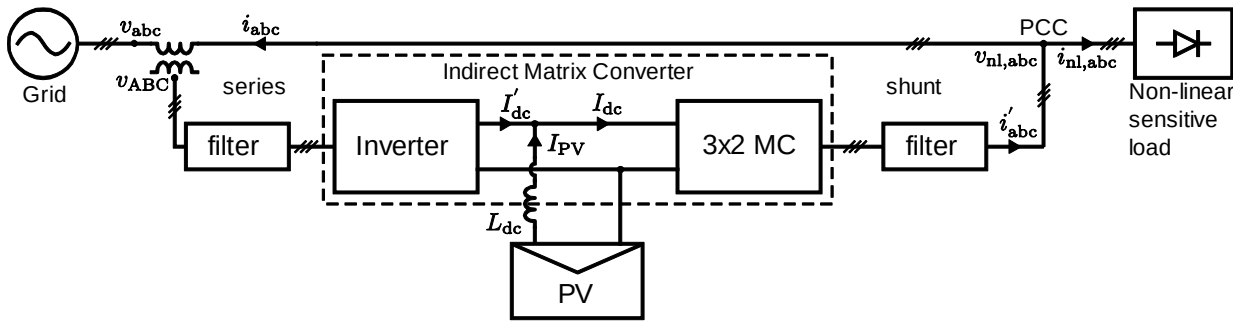

Figure 1. Indirect Matrix Converter-based Unified Power Quality Conditioner with the PV array inserted in the DC link

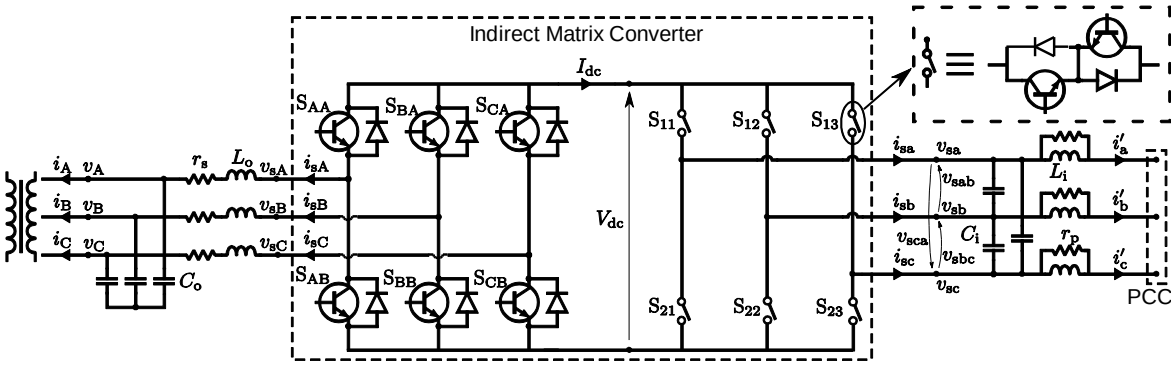

Figure 2. Detailed representation of the Indirect Matrix Converter and the filters

TABLE I. SWITCHING STATES OF THE SERIES CONVERTER WITH THE SWITCHES CONDUCTING ON THE FIRST **(1)**, SECOND **(2)** AND THIRD **(3)** LEGS, WITH THEIR EFFECT ON DC CURRENT AND AC VOLTAGES

S	(1)	(2)	(3)	I_{dc}	v_{sAB}	v_{sBC}	v_{sCA}	$\|\vec{v}_s\|$	$\arg(\vec{v}_s)$
1	S_{AA}	S_{BB}	S_{CB}	$-i_A$	V_{dc}	0	$-V_{dc}$	$\sqrt{2/3}V_{dc}$	0
2	S_{AA}	S_{BA}	S_{CB}	i_C	0	V_{dc}	$-V_{dc}$	$\sqrt{2/3}V_{dc}$	$\pi/3$
3	S_{AB}	S_{BA}	S_{CB}	i_B	$-V_{dc}$	V_{dc}	0	$\sqrt{2/3}V_{dc}$	$2\pi/3$
4	S_{AB}	S_{BA}	S_{CA}	$-i_A$	$-V_{dc}$	0	V_{dc}	$\sqrt{2/3}V_{dc}$	π
5	S_{AB}	S_{BB}	S_{CA}	i_C	0	$-V_{dc}$	V_{dc}	$\sqrt{2/3}V_{dc}$	$-2\pi/3$
6	S_{AA}	S_{BB}	S_{CA}	i_B	V_{dc}	$-V_{dc}$	0	$\sqrt{2/3}V_{dc}$	$-\pi/3$
7	S_{AA}	S_{BA}	S_{CA}	0	0	0	0	0	-
8	S_{AB}	S_{BB}	S_{CB}	0	0	0	0	0	-

frame αβ, delimiting the six voltage zones over one grid period. The inverter reference voltage vector $\vec{v}_r$ is also shown with its angle θ_i in relation to the previous switching space vector. Similarly, the actual inverter voltage vector is denoted by $\vec{v}_2 = \|\vec{v}_2\| \angle \theta_2$, with $\|\vec{v}_r\| = \sqrt{3}V_2 = \sqrt{3/2}\hat{V}_2$.

In order to reproduce the inverter reference voltage, the two closest space vectors are applied alternatively with zero vectors. For example, in zone I the switching vectors 1 and 2 are applied alternatively with the zero vector 7 or 8. Referring to these two vectors with the indices α and β, and considering the six voltage zones of π/3, the duty cycles are obtained with

$$d_\alpha = m_2 \sin(\pi/3 - \theta_i) \;,\; d_\beta = m_2 \sin\theta_i \,, \tag{8}$$

where $m_2 = \sqrt{3}\hat{V}_2 / V_{dc}$ is the modulation index (max. value of 1). Zero vectors are used during the rest of the switching period with a combined duty cycle $d_0 = 1 - (d_\alpha + d_\beta)$.

The voltage vector is obtained based on the above duty

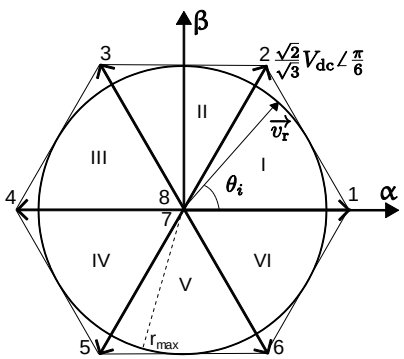

Figure 3. Voltage space vectors of the series inverter

TABLE II. SWITCHING STATES OF THE SHUNT CONVERTER WITH THE SWITCHES CONDUCTING ON THE UPPER **(1)** AND LOWER **(2)** BRANCHES, WITH THEIR EFFECT ON DC VOLTAGE AND AC CURRENTS

S	(1)	(2)	V_{dc}	i_{sa}	i_{sb}	i_{sc}	$\|\vec{i}_s\|$	$\arg(\vec{i}_s)$
1	S_{11}	S_{22}	v_{sab}	I_{dc}	$-I_{dc}$	0	$\sqrt{2}I_{dc}$	$-\pi/6$
2	S_{12}	S_{21}	$-v_{sab}$	$-I_{dc}$	I_{dc}	0	$\sqrt{2}I_{dc}$	$5\pi/6$
3	S_{12}	S_{23}	v_{sbc}	0	I_{dc}	$-I_{dc}$	$\sqrt{2}I_{dc}$	$\pi/2$
4	S_{13}	S_{22}	$-v_{sbc}$	0	$-I_{dc}$	I_{dc}	$\sqrt{2}I_{dc}$	$-\pi/2$
5	S_{11}	S_{23}	$-v_{sca}$	I_{dc}	0	$-I_{dc}$	$\sqrt{2}I_{dc}$	$\pi/6$
6	S_{13}	S_{21}	v_{sca}	$-I_{dc}$	0	I_{dc}	$\sqrt{2}I_{dc}$	$-5\pi/6$
7	S_{11}	S_{21}	0	0	0	0	0	-
8	S_{12}	S_{22}	0	0	0	0	0	-
9	S_{13}	S_{23}	0	0	0	0	0	-

cycles. Considering zone I, it results in (9).

$$\begin{aligned} \vec{v}_2 &= d_\alpha \vec{v}_{s1} + d_\beta \vec{v}_{s2} \\ &= m_2 \sqrt{2/3} V_{dc} \left(\sin(\pi/3 - \theta_i) + \sin\theta_i e^{i\pi/3} \right) \end{aligned} \tag{9}$$

The amplitude of the voltage vector is therefore constant for a constant modulation index, with a value of $\|\vec{v}_2\| = m_2 V_{dc}/\sqrt{2}$, as shown in Fig. 3 where the vector rotates following the circle that has a maximum radius r_{max} of $V_{dc}/\sqrt{2}$ when $m_2 = 1$. As a result, the amplitude of the AC voltages defined in (7) is

$$\hat{V}_2 = m_2 V_{dc} / \sqrt{3} \,, \tag{10}$$

with a maximum value of $V_{dc}/\sqrt{3}$.

As shown in Table I, the instantaneous DC link current is determined by the switching vector used. Its average value over a commutation period of the series inverter $T_{sw,2}$ can be expressed with a combination of the switching vectors and their respective duty cycles. For example, considering zone 1 and therefore the switching vectors 1 and 2, it results in (11).

$$I_{dc,0} = m_2 \left(\sin(\pi/3 - \theta_i)(-i_A) + \sin\theta_i i_C \right) \tag{11}$$

Considering the series inverter AC currents defined in (7) and the average value of the DC link voltage over $T_{sw,2}$, the current in the DC link is obtained in (12).

$$I_{dc,0} = -\frac{3}{2} \frac{\hat{V}_2}{V_{dc,0}} \hat{I}_2 \cos\phi_2 \tag{12}$$

B. Shunt converter modulation

The modulation of the shunt converter is discussed in [12] and [13] where two SVM with PWM methods are proposed: 'maximum DC voltage modulation' and 'reduced DC voltage modulation'. The latter has the advantage of featuring a lower DC voltage with reduced commutation losses in the series inverter. However, the utility of this voltage in the system proposed here is twofold: it is the voltage used both by the series inverter and to control the PV array current, which is why the maximum DC voltage modulation must be used (see next sections). As a first approach, the converter is considered with a constant DC current source.

The AC current vectors are obtained in Table II in function of the switching vectors, and are also represented by space vectors $\vec{i}_s$, shown in Fig. 4 in the two-axis non-rotating frame αβ. The 3x2 MC reference current space vector $\vec{i}_r$ is shown with its angle θ_r in relation to the previous space vector and its absolute angle θ. The actual space vector is denoted by $\vec{i}_1$.

With maximum DC voltage modulation, the two closest vectors to the reference one are alternatively applied, most commonly with no zero vector [12], [13], resulting in two different voltage levels in the DC link within each modulation period. Considering Table II, each AC current can be expressed in function of the switching vectors duty cycles in a certain zone. For example in zone II we have

$$i_{sa} = d_{S5} I_{dc} \ , \ i_{sb} = d_{S3} I_{dc} \ , \ i_{sc} = -\left(d_{S5} + d_{S3}\right) I_{dc} , \qquad (13)$$

with $d_{S5} + d_{S3} = 1$. This results in the duty cycles

$$d_{S5} = -\frac{i_{sa}}{i_{sc}} = -\frac{v_a}{v_c} \ , \ d_{S3} = -\frac{i_{sb}}{i_{sc}} = -\frac{v_b}{v_c} , \qquad (14)$$

aiming at a unitary Displacement Power Factor (DPF) and thus $\phi_1 = 0$, that is the AC current targets are in phase with and proportional to the grid voltages defined in (6). Expressing these duty cycles in function of the angle θ_r of the reference current vector for each voltage zone, we obtain (15), where $d_\gamma = \sin\left(\pi/3 - \theta_r\right)$ and $d_\delta = \sin\theta_r$ [12].

$$d_1 = \frac{d_\gamma}{d_\gamma + d_\delta} \ , \ d_2 = \frac{d_\delta}{d_\gamma + d_\delta} \qquad (15)$$

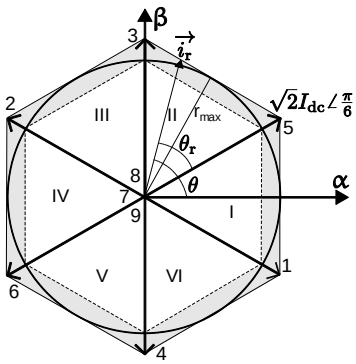

Figure 4. Current space vectors (maximum DC voltage modulation) in the αβ frame with representation of the hexagonal and circular paths followed by the AC current vector in case of zero vector-free and zero vector modulations, respectively

This approach where no zero vectors are used and therefore the sum of the duty cycles is equal to 1 does not allow controlling the amplitude of the AC currents. The average current space vector formed over a modulation period is defined by the duty cycles and follows a hexagon whose outer circle radius is $\sqrt{2}I_{dc}$ and corresponds to the amplitude of the switching vectors, as shown in Fig. 4—this means that its amplitude is not constant. In each voltage zone it varies with $\cos\left(\pi/6 - \theta_r\right)$, such that

$$\left\|\vec{i}_r\right\| = \frac{\sqrt{3}}{\sqrt{2}} \frac{I_{dc}}{\cos\left(\pi/6 - \theta_r\right)} \ . \qquad (16)$$

Thus, the AC currents are not sinusoidal if the average value of the DC link current is constant.

This justifies the consideration of a modulation method where the sum of the duty cycles is not constant and zero vectors are used. It is a similar method to the one used for the series inverter and the duty cycles are simply $d_1 = m_1 d_\gamma$ and $d_2 = m_1 d_\delta$, where $m_1 = \sqrt{2}\left\|\vec{i}_r\right\| / \sqrt{3} I_{dc,0}$ allows controlling the amplitude of the grid currents using the average value of the DC link current over the running commutation period of the series inverter $T_{sw,2}$. The zero vectors are therefore applied during a duty cycle of $d_{off} = 1 - \left(d_1 + d_2\right)$.

The AC current vector is obtained as a combination of the two closest space vectors. In zone I, this results in (17).

$$\begin{aligned} \vec{i}_1 &= d_1 \vec{i}_{s1} + d_2 \vec{i}_{s5} \\ &= m_1 \sqrt{2} I_{dc} \left(\sin\left(\pi/3 - \theta_r\right) e^{-i\pi/6} + \sin\theta_r e^{i\pi/6}\right) \end{aligned} \qquad (17)$$

The amplitude results in a constant value of

$$\left\|\vec{i}_1\right\| = \frac{\sqrt{3}}{\sqrt{2}} m_1 I_{dc} , \qquad (18)$$

which generates sinusoidal grid currents whose amplitude can be adjusted with lower values of m_1. The amplitude of the AC currents defined in (6) is $\hat{I}_1 = m_1 I_{dc}$.

If the maximum allowed current space vector is considered with $m_1 = 1$, the path of the vector $\vec{i}_1$ and its reference $\vec{i}_r$ follows the circle in Fig. 4 with a radius equal to

$$r_{max} = \left\|\vec{i}_r\right\|_{max} = \frac{\sqrt{3}}{\sqrt{2}} I_{dc,0} \ . \qquad (19)$$

With the first modulation method (no zero vectors and a constant sum of duty cycles), the DC link voltage averaged over a switching period of the shunt converter $T_{sw,1}$ (zone I) is

$$V_{dc,0} = \frac{d_\gamma}{d_\gamma + d_\delta} v_{ab} + \frac{d_\delta}{d_\gamma + d_\delta} \left(-v_{ca}\right) \ . \qquad (20)$$

Using the expressions of the duty cycles and knowing that $\theta_r = \theta + \pi/6$ in zone I, we obtain

$$V_{dc,0} = \frac{3}{2} \frac{\hat{V}_1}{d_\gamma + d_\delta} = \frac{3}{2} \frac{\hat{V}_1}{\cos\left(\pi/6 - \theta_r\right)} \ , \qquad (21)$$

which is valid for any zone considered and shows a variation with six times the grid frequency. Similarly, when zero vectors are considered with non-constant duty cycles, we have

$$V_{\mathrm{dc},0} = \frac{3}{2} m_1 \hat{V}_1 = \frac{3}{2} \frac{\hat{I}_1}{I_{\mathrm{dc},0}} \hat{V}_1 , \tag{22}$$

where the average value of the DC link current over any commutation period of the series converter in (12) is considered for generalization and further considerations. This expression is similar to the one obtained in (12) except that the DC voltage is not averaged over the same period in both cases.

C. Indirect Matrix Converter modulation

When considering the whole IMC, the DC link voltage resulting from the 3x2 MC and the DC link current resulting from the series inverter are used to form the compensating series voltages and shunt currents, respectively. Thus, the modulations of the shunt and series converters should be properly synchronized. There are two different and variable commutation periods of the series converter ($T_{\mathrm{sw},2}$) inside each of the shunt converter ones ($T_{\mathrm{sw},1}$ or T_{sw}).

1) Combination of input and output converters: The discussion about the path of the shunt current space vector has to be considered here taking into account the local average DC link current obtained from the series inverter in (12). The expression has to be adapted in function of the local average DC link voltages obtained for the two shunt converter modulation methods in (21) and (22).

With the no-zero-vector modulation method, the average DC link current over $T_{\mathrm{sw},1}$ reads:

$$I_{\mathrm{dc},0} = -\frac{\hat{V}_2}{\hat{V}_1} \hat{I}_2 \cos\phi_2 \cos(\pi/6 - \theta_2) , \tag{23}$$

using the average DC link voltage over the same switching period. The current varies with six times the grid frequency, which results in a shunt converter current space vector of constant amplitude in (16), that generates sinusoidal AC currents with non-controllable amplitude:

$$\left\| \vec{i}_{\mathrm{r}} \right\| = \frac{\sqrt{3}}{\sqrt{2}} \frac{I_{\mathrm{dc},0}}{\cos(\pi/6 - \theta_{\mathrm{r}})} = \frac{\sqrt{3}}{\sqrt{2}} \frac{\hat{V}_2}{\hat{V}_1} \hat{I}_2 \cos\phi_2 \ . \tag{24}$$

The maximum voltage transfer ratio between the shunt and series sides of the IMC ($\hat{V}_1$ and $\hat{V}_2$), considering (10) and (21) with m_2 varying between $\cos(\pi/3)$ and 1 (guaranteeing a constant value for $\hat{V}_2$), is $\sqrt{3}/2$.

With the zero-vector modulation method, a constant AC current vector can be obtained regardless of the variation of $I_{\mathrm{dc},0}$: the modulation index is set to

$$m_1 = \sqrt{2} \left\| \vec{i}_{\mathrm{r}} \right\| / \sqrt{3} I_{\mathrm{dc},0} \tag{25}$$

and has opposite dynamics to $I_{\mathrm{dc},0}$.

When using zero vectors, the maximum voltage transfer ratio between both sides of the IMC depends on the modulation index of the shunt converter as the sum of the duty cycles is not constant. This can be an issue and justifies the common use of the no-zero-vector modulation method in IMCs [12], [13]. However, the situation is different when introducing the PV array in the DC link and zero vectors are necessary.

2) Switching sequence: The duty cycles are synchronized for the whole IMC, such that each switching sequence of the series converter takes place during a constant non-zero switching state of the shunt converter. The zero-vector method for the shunt converter is considered (see next section), but the sequence remains similar in case no zero vectors are used.

The switching sequence of the IMC is represented in Fig. 5 with the respective duty cycles of the shunt and series converters over one switching period T_{sw}. The duty cycles of the series inverter depend on the DC-link voltage—their absolute values within a complete IMC switching period are given by (26) and (27), where the relative duty cycles d^{r} are obtained from (8).

$$d_{\alpha 1} = \frac{d_1}{d_1 + d_2} d^{\mathrm{r}}_{\alpha 1} \ , \ d_{\alpha 2} = \frac{d_2}{d_1 + d_2} d^{\mathrm{r}}_{\alpha 2} \tag{26}$$

$$d_{\beta 1} = \frac{d_1}{d_1 + d_2} d^{\mathrm{r}}_{\beta 1} \ , \ d_{\beta 2} = \frac{d_2}{d_1 + d_2} d^{\mathrm{r}}_{\beta 2} \tag{27}$$

The on-time of the series inverter zero vectors are adapted to the switching periods of the 3x2 MC:

$$d_{01} = d_1 - (d_{\alpha 1} + d_{\beta 1}) \ , \ d_{02} = d_2 - (d_{\alpha 2} + d_{\beta 2}) , \tag{28}$$

with $d_0 = d_{\mathrm{off}} + d_{01} + d_{02}$. The duty cycles of the shunt converter remain the same, and non-zero vectors are used during a time $t_{\mathrm{on}} = (d_1 + d_2) T_{\mathrm{sw}}$. In particular, when zero vectors are used (during $t_{\mathrm{off}} = T_{\mathrm{sw}} - t_{\mathrm{on}}$), the converter is off and zero vectors are applied to the series inverter as well.

The zero vectors of the series inverter are applied during the switching of the 3x2 MC to allow for soft switching operation and lower losses [12], [13]. The DC link variables are shown in Fig. 6, considering that $d_{\mathrm{off}} = 0$ (no zero vectors for the shunt converter), with the same numbers as in Fig. 5 for the commutation of the converters.

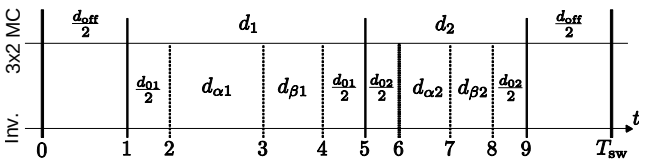

Figure 5. Switching sequence of the shunt and series converters with their respective duty cycles

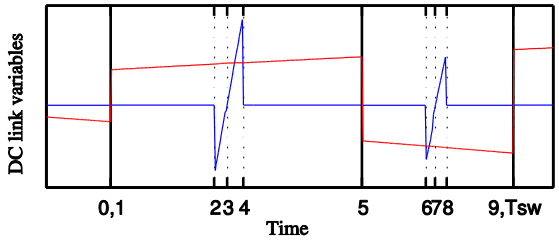

Figure 6. DC link variables during a switching sequence of the IMC: voltage in red and current in blue

D. With PV array

The topology is here considered adding the PV array in parallel in the DC link of the IMC, as in Fig. 1. A constant current source is first considered to represent the PV array. The objective is to obtain sinusoidal shunt converter AC currents or a constant current space vector. The introduction of the current source does not affect the DC link voltage and the series inverter modulation does not require any reconsideration. The DC link current of the shunt converter $I_{\rm dc}$ is expressed by (3) and, considering that nearly all the power flows through the shunt converter, $I_{\rm dc}^{'}$ is not affected by the introduction of the current source.

Using the no-zero-vector modulation, the constant current source component generates a non-constant AC current vector, as shown in (16). The proposed solution is to use the zero-vector modulation introduced above. The equations obtained for the shunt and series converters and the IMC remain valid if considering (3), which is also given by

$$I_{\rm dc,0} = I_{\rm PV} - \frac{3}{2}\frac{\hat{V}_2}{V_{\rm dc,0}}\hat{I}_2\cos\phi_2 \ . \tag{29}$$

The modulation index of the shunt converter defined in (25) follows these dynamics to reproduce sinusoidal AC currents. However, $I_{\rm dc,0}^{'}$ is expected to be much smaller than $I_{\rm PV}$, which is why we consider that $I_{\rm dc} \simeq I_{\rm PV}$. The equations in Section III-B, with a constant DC source, are valid as is.

As a conclusion, a zero-vector modulation method is chosen for the shunt converter as it produces sinusoidal AC currents with controllable amplitude based on a dominant DC component in the 'virtual DC link'. The additional control of the PV array current is detailed in the next section.

IV. Control of the System

The control of the IMC provides adequate voltage and current vectors for the series and shunt converter modulations, respectively, so as to compensate the voltage harmonics, sags and swells, mitigate the current harmonics and guarantee a nearly unitary DPF. Also, the DC link voltage control from the shunt converter regulates the PV array operating point.

The control is done in the synchronously rotating *dq* frame, using the power-invariant Park-Concordia transformation, which leads to reference vectors in (30).

$$\vec{x}_{\rm r} = \sqrt{x_d^2 + x_q^2}\angle\tan\frac{x_q}{x_d} \tag{30}$$

A. Shunt converter control

The shunt converter is controlled for reactive current compensation or DPF regulation, current harmonics mitigation and PV array current control. In order to simplify the circuit and avoid extra measurements, the feedback is applied directly on the grid currents, and the shunt converter AC currents are not measured [2]. This results in the control circuit in Fig. 7, where the *d* and *q* components of the grid currents are controlled using a PID controller with a plug-in repetitive controller for improved dynamics.

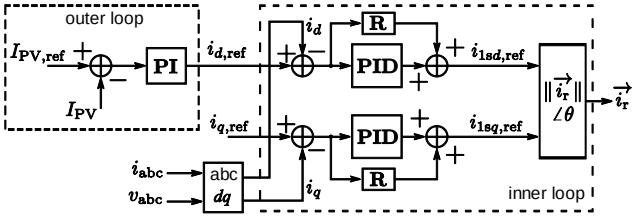

Figure 7. Control circuit of the PV array current (outer loop) and the grid currents (inner loop) outputting the reference current vector for the shunt converter modulation

The reactive current compensation or the nearly unitary DPF is accomplished by choosing a reference value of $i_q = 0$ at the input of the inner control loop where a feedback is applied on the grid currents.

The non-linear load current harmonics mitigation is guaranteed by controlling the *d* component of the grid currents to be constant. The reference can be generated with the control of the PV array current, as they are linked by the modulation of the DC link voltage; this consists in the outer control loop.

The control of the DC link voltage also allows controlling the PV array current $I_{\rm PV}$:

$$V_{\rm PV} - V_{\rm dc} = L_{\rm dc}\frac{{\rm d}I_{\rm PV}}{{\rm d}t}\ , \tag{31}$$

which implies that $I_{\rm PV}$ increases when $V_{\rm PV} > V_{\rm dc}$, and vice versa. Using no zero vectors, the situation where $V_{\rm PV} > V_{\rm dc}$ cannot be guaranteed. With this modulation method, however, the zero vectors are used to increase $I_{\rm PV}$. Also, the maximum DC link voltage modulation is necessary to have $V_{\rm dc} > V_{\rm PV}$ for any non-zero vector. The grid currents are the controlled variables, which leads to the following dynamics: if $I_{\rm PV}$ should be increased, then the on-time of the zero vectors of the shunt converter should be increased, that is the average DC link voltage and the reference amplitude of the AC current vector should be decreased, as shown in Table III [2]. Therefore, the PV array current or voltage can be controlled based on the DC link voltage modulation and the shunt converter current reference.

B. Series converter control

The series converter AC voltages are controlled so as to compensate the distortions in the grid voltages (harmonics, sags or swells) and supply sinusoidal voltages to the loads, following (1). Their references can thus be obtained with (32), where $v_{\rm abc,ref}$ are the reference sinusoidal grid voltages [4].

$$v_{\rm ABC,ref} = v_{\rm abc,ref} - v_{\rm abc} \tag{32}$$

The series converter voltages are then controlled with a PI controller generating the reference vector for the modulator.

TABLE III. Relations for the Control of the PV Array Current

$\|\vec{i}_{\rm i1}\|$	$V_{\rm dc,0}$	$V_{\rm L}$	$I_{\rm PV}$	$V_{\rm PV}$	${\rm d}P/{\rm d}V$	$P_{\rm PV}$
↗	$> V_{\rm PV}$	< 0	↘	↗	> 0	↗
					< 0	↘
↘	$< V_{\rm PV}$	> 0	↗	↘	> 0	↘
					< 0	↗

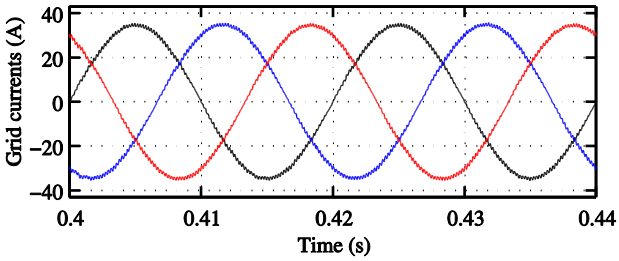

Figure 8. Grid currents in normal operation – THD = 2.33 %

V. SIMULATION RESULTS

The complete system in Fig. 1 is simulated in the MATLAB/Simulink environment, with the parameter values in Table IV. The PV array voltage is limited by the step-up capability of the converter (it has to be lower than the lowest DC link voltage during non-zero-vector operation) and the system is considered to work at Maximum Power Point (MPP) in rated conditions, with a current $I_{PV} = 50\text{A}$ and a voltage $V_{PV} = 370\text{V}$. The grid currents in these conditions are shown in Fig. 8 with a Total Harmonic Distortion (THD) of 2.33 %.

A. *Non-linear load current harmonics*

The non-linear load connected at the Point of Common Coupling (PCC) is simulated using a three-phase full-bridge diode rectifier consuming a power of 5 kW. The load currents are shown in Fig. 9a with a THD of 22.25 % and particularly high 5^{th} and 7^{th} harmonics of 20.30 % and 7.83 % of the fundamental, respectively. The compensated grid currents in Fig. 9b have a THD of 4.13 %—2.71 % when considering only the first 40 harmonics—and the 5^{th} and 7^{th} harmonics are attenuated to 1.43 % and 1.87 % of the fundamental, respectively. The compensating shunt converter AC currents in Fig. 9c present clearly the load harmonics.

B. *Grid voltages sag and swell*

The PV array is considered with an irradiance of 0.5 kW/m², still at MPP, resulting in a current $I_{PV} = 25\text{A}$ and a voltage $V_{PV} = 359\text{V}$. The grid voltages are shown in Fig. 10a with a 25 % sag and then a 10 % swell during 4 grid periods

TABLE IV. SIMULATION PARAMETER VALUES

Symbol	Description	Value	Units
T_s	Sample time	14	µs
f_{sw}	Switching frequency of the IMC	4.8	kHz
v	Grid phase rms voltage	230	V
f_g	Grid frequency	50	Hz
a	Series transformer turns ration	1:4	-
P_{PV}	PV array nominal power	18.5	kW
L_{dc}	PV array output inductance	12	mH
C_i	Shunt filter line-to-line capacitance (Δ)	10	µF
L_i	Shunt filter phase inductance	2	mH
r_p	Shunt filter damping resistance	40	Ω
C_0	Series filter phase capacitance	30	µF
L_0	Series filter phase inductance	4	mH
r_s	Series filter resistance	10	Ω

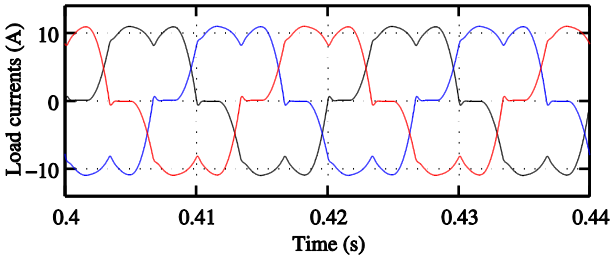

a. Load currents – $THD_{40} = 22.25\%$

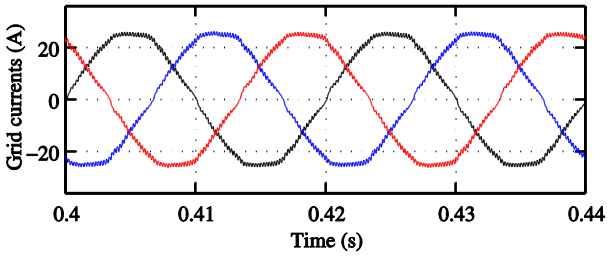

b. Grid currents – $THD_{40} = 2.71$ %

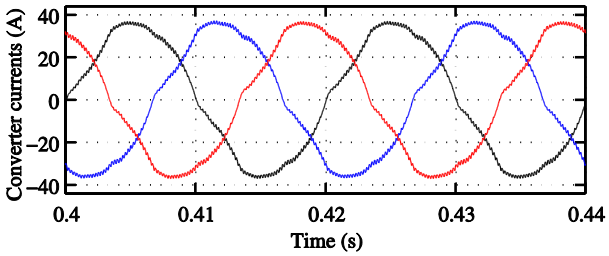

c. Shunt converter AC currents – $THD_{40} = 6.00$ %

Figure 9. Simulation results of the system in nominal conditions with a non-linear load of 5 kW connected at the PCC

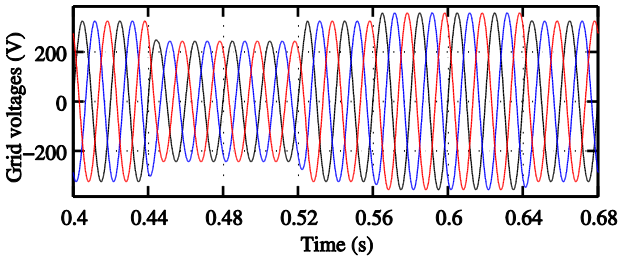

a. Grid voltages

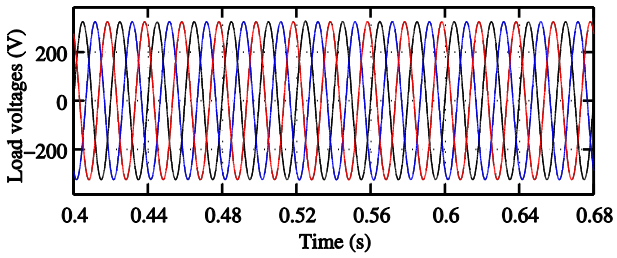

b. Load voltages with their references

Figure 10. Simulation results with sag and swell in the grid voltages

each (from 0.44 s to 0.52 s and from 0.56 s to 0.64 s, respectively). The load voltages in Fig. 10b confirm that the series voltage compensation works fine as they follow their reference for a constant amplitude. Also, the grid currents remain unaffected with a THD of 2.61 % during the sag.

C. *Grid voltages harmonics*

The grid voltages in Fig. 11a have 5th and 7th harmonics of 3.5 % and 2.5 % of the fundamental, respectively, and a THD of 4.30 %, in rated conditions. These are compensated by the series inverter voltages to result in the nearly sinusoidal load voltages in Fig. 11b with a 5th and a 7th harmonic of 0.47 % and 0.59 %, respectively, and a THD of 0.88 %.

VI. CONCLUSION

This paper has presented the development of a PV system using a UPQC-based topology with the use of an IMC allowing the connection of a PV array in the 'virtual DC link'. Current- and voltage-related PQ issues such as current harmonics and voltage sags, swells and harmonics have been tackled in addition to the usual MPPT and unitary PF ones. A modulation method has been proposed in order to allow the connection of a PV array. In particular, the DC link voltage modulation has been evaluated as it is used to control the PV array current, the grid currents and the series converter compensation voltage. Simulations in MATLAB/Simulink confirm the system properly mitigates the abovementioned PQ issues.

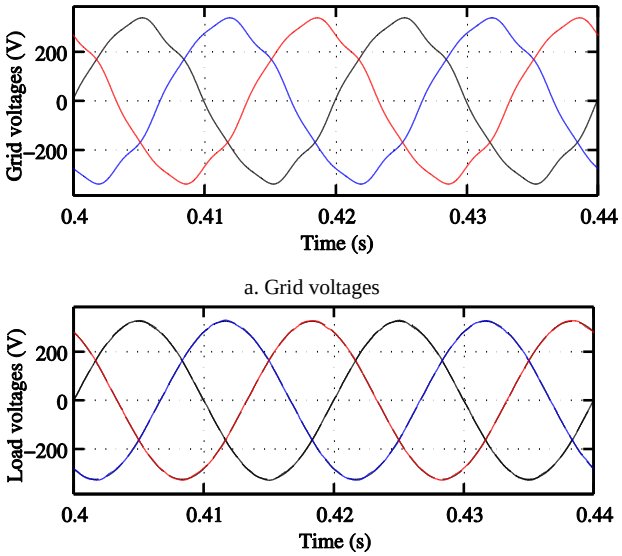

a. Grid voltages

b. Load voltages with their references

Figure 11. Simulation results with harmonics in the grid voltages

ACKNOWLEDGMENT

Thomas Geury would like to thank the Belgian Fund for training in Research in Industry and in Agriculture (F.R.I.A.) for the funding of this research project. This work was supported by national funds through Fundação para a Ciência e Tecnologia (FCT) with reference UID/CEC/50021/2013.

REFERENCES

[1] R. Teodorescu, M. Liserre, and P. Rodriguez, *Grid converters for photovoltaic and wind power systems*. United Kingdom: John Wiley & Sons, Ltd., 2011.

[2] T. Geury, S. Pinto, and J. Gyselinck, "Current source inverter-based photovoltaic system with enhanced active filtering functionalities," *IET Power Electron.*, p. 9, 2015 (online August 2015).

[3] V. Khadkikar, "Enhancing electric power quality using upqc : a comprehensive overview," *IEEE Trans. Power Electron.*, vol. 27, no. 5, pp. 2284–2297, 2012.

[4] B. Han, B. Bae, H. Kim, and S. Baek, "Combined operation of unified power-quality conditioner with distributed generation," *IEEE Trans. Power Deliv.*, vol. 21, no. 1, pp. 330–338, 2006.

[5] G. Tsengenes, G. A. Adamidis, and A. D. Karlis, "Improving the voltage profile of a medium voltage grid using distributed generation units," in *15th European Conference on Power Electronics and Applications*, 2013, pp. 1–9.

[6] R. A. Mastromauro, M. Liserre, and A. D. Aquila, "Single-phase grid-connected photovoltaic systems with power quality conditioner functionality," in *European Conference on Power Electronics and Applications*, 2007, pp. 1–11.

[7] M. Taghizadeh, J. Sadeh, and E. Kamyab, "Protection of grid connected photovoltaic system during voltage sag," *2011 Int. Conf. Adv. Power Syst. Autom. Prot.*, pp. 2030–2035, Oct. 2011.

[8] X. Chen, Q. Fu, S. Yu, and L. Zhou, "Unified control of photovoltaic grid-connection and power quality managements," in *Workshop on Power Electronics and Intelligent Transportation System*, 2008, pp. 360–365.

[9] P. Wheeler, J. Rodríguez, J. C. Clare, L. Empringham, and A. Weinstein, "Matrix converters : a technology review," *IEEE Trans. Ind. Electron.*, vol. 49, no. 2, pp. 276–288, 2002.

[10] J. Ferreira and S. Pinto, "P-Q decoupled control scheme for unified power flow controllers using sparse matrix converters," in *5th International Conference on the European Electricity Market*, 2008, no. 1, pp. 1–6.

[11] P. Correa, J. Rodríguez, M. Rivera, J. R. Espinoza, and J. W. Kolar, "Predictive control of an indirect matrix converter," *IEEE Trans. Ind. Electron.*, vol. 56, no. 6, pp. 1847–1853, 2009.

[12] R. Peña, R. Cárdenas, E. Reyes, J. Clare, and P. Wheeler, "Control of a doubly fed induction generator via an indirect matrix converter with changing dc voltage," *IEEE Trans. Ind. Electron.*, vol. 58, no. 10, pp. 4664–4674, 2011.

[13] J. W. Kolar, M. Baumann, F. Schafmeister, and H. Ertl, "Novel three-phase ac-dc-ac sparse matrix converter - part i : derivation, basic principle of operation, space vector modulation, dimensioning," in *Applied Power Electronics Conference and Exposition*, 2002, pp. 777–791.

[14] S. Raju and N. Mohan, "Space vector modulated hybrid indirect multilevel matrix converter," in *39th Annual Conference of the IEEE Industrial Electronics Society*, 2013, pp. 4931–4936.

[15] P. Petrowitsch et al., "Predictive voltage control with imposed source current waveforms in an indirect matrix converter," in *39th Annual Conference of the IEEE Industrial Electronics Society*, 2013, pp. 4907–4912.

[16] M. Chai, R. Dutta, and J. Fletcher, "Space vector pwm for three-to-five phase indirect matrix converters with d2-q2 vector elimination," in *39th Annual Conference of the IEEE Industrial Electronics Society*, 2013, pp. 4937–4942.